Interacting spinless fermions with disorder: the Mott transition for infinite coordination number

1993 J. Phys.: Condens. Matter 5 2561

(http://iopscience.iop.org/0953-8984/5/16/014)

J. Phys.: Condens. Matter 5 (1993) 2561–2582. Printed in the UK

Interacting spinless fermions with disorder: the Mott transition for infinite coordination number

G S Uhrig and R Vlaming

Institut für Theoretische Physik C, Technische Hochschule Aachen, D-5100 Aachen, Federal Republic of Germany

Received 4 December 1992

Abstract. An analytic expression for the dynamical conductivity $\sigma(\omega)$ of spinless fermions with local disorder and nearest-neighbour repulsion is derived on lattices with infinite coordination number Z. The model is *exactly* solvable in the whole parameter range assuming two possible phases: a homogeneous phase and a checkerboard charge-density wave (CDW). Away from half filling the system displays anomalous behaviour: weak particle-density fluctuations favour spontaneous symmetry breaking. First, we investigate the effects of this anomaly on the conductivity in the AC and DC regimes. Second, we focus on the Mott transition occurring at zero temperature at half filling. The critical exponents for the conductivity are computed for the dependence on the interaction U, the disorder γ, the filling n, the temperature T and the frequency ω.

1. Introduction

Itinerant quantum systems with strong correlations are one of the important subjects of condensed matter theory. Interaction and disorder are the two main sources of correlation. This research field is very active [1–9], for a review see [10], but the full interplay between interaction and disorder effects is far from being completely understood. The main part of recent investigations considers interacting models containing spin degrees of freedom (e.g. the Hubbard model). The formation of local magnetic moments [6, 7] poses serious problems in the investigation of such models. In the application of renormalization group techniques this effect hinders the description of the metal–insulator transition (MIT) because the magnetic effects occur before the MIT is reached [7–9].

Since no exact solution of a disordered itinerant quantum model is available for dimensions $d > 1$, we turn to the construction of a comprehensive mean-field theory capable of treating disorder *and* interaction on an *equal* footing. Recently it has been found that such a mean-field theory is provided by the solution of a lattice model in the limit of high coordination number Z [11, 12], which was introduced for itinerant quantum models in [13], for a review see [14]. The solution, however, of a Hubbard-like model with or without disorder in the limit $Z \to \infty$ is still an extremely complicated problem, which can be tackled at present only by means of QMC simulations [5, 15–18]. The results obtained by this method do not yet yield a consistent picture of the MIT.

The situation is much clearer for a model of spinless fermions, i.e. a model allowing only for one kind of fermion per site. We consider fermions that interact repulsively on neighbouring sites (a screened Coulomb interaction); disorder is included by randomly distributed local energies. Here an *exact* solution in the limit $Z \to \infty$ is available. We refer

0953-8984/93/162561+22$07.50

the reader to a previous paper [12]†, which we will designate in the rest of the paper by [VUV].

To abandon the spin degrees of freedom is certainly a serious restriction. The charge degrees of freedom, however, are responsible for the electric current so that a MIT can be investigated. A detailed knowledge of this simpler scenario is certainly of great help in understanding the MIT in more complex systems with spin. Moreover, spinless fermions provide a model in their own right for the description of strongly polarized systems, as well as for ferromagnetic (or ferrimagnetic) systems where one spin band is completely filled and only the other has to be dealt with (e.g. magnetite Fe_3O_4, as first suggested in [19]).

In one dimension the model of spinless fermions without disorder is solved exactly by means of a Bethe ansatz [20,21]. At half filling the ground state passes from a homogeneous phase to a charge-density ordered phase at a *finite* value of the interaction. This turns out to be a peculiarity of $d = 1$ [22]. In infinite dimensions, $d \to \infty$, the interaction enters in a diagrammatic expansion only via the Hartree diagram [23], and spontaneous symmetry breaking occurs for an infinitesimally small interaction at half filling [VUV]. Without interaction, but with disorder, the infinite-dimensional system is solvable; the solution is equivalent to the equations of the coherent-potential approximation [24].

The system with both interaction and disorder displays a transition at finite interactions [VUV]. The transition implies band splitting, which induces a metal–insulator transition at half filling. Since it is induced by the interaction it represents an example of a *Mott transition*. Away from half filling we found that in a certain parameter range the critical interaction is *anomalously lowered* by small particle-density fluctuations due to disorder and/or temperature.

In the present paper we will give an analytic description of the dynamical conductivity of spinless fermions in the limit $Z \to \infty$ in the whole parameter range (interaction, disorder, temperature, filling). It will be based on the one-particle properties presented in [VUV]. We find that vertex corrections do not contribute; they are suppressed by the limit $Z \to \infty$. In the Hubbard model without disorder this has been shown in [25]. Our calculations are formally performed for the Bethe lattice and on an appropriately defined periodic extension of this lattice that allows a canonical definition of transport. The results, however, depend on the lattice structure only via the free density of states, which is half-elliptic for the Bethe lattice in $Z \to \infty$. Therefore, we would like to emphasize that our calculations can equally be done for any other DOS. In particular, one could use the DOS for the three-dimensional simple cubic lattice.

We investigate the effects of the anomaly on the conductivity away from half filling. It turns out that in the anomalous region the DC conductivity is larger for lower temperature. The same effect occurs in the dependence on the disorder, but is less clearly visible. In the AC conductivity, also, the peak structure due to the energy gap vanishes anomalously on lowering of the temperature/disorder in a certain parameter region. Furthermore, we examine the Mott transition at half filling, computing the dependence of the DC conductivity on various parameters: interaction, disorder, doping and temperature. We calculate all the corresponding critical exponents.

The present paper is set out as follows. In section 2 the Hamilton operator and the lattice are introduced. In addition we recall essential results of our previous paper [VUV]. The necessary formalism to calculate a transport coefficient is presented in section 3; the

† Unfortunately in this paper figures 9, 10 and 11 were printed in the wrong order. Correctly, the plot of figure 9 belongs to the caption of figure 11, the plot of figure 10 to the caption of figure 9 and the plot of figure 11 to the caption of figure 10; see also the erratum *J. Phys.: Condensed Matter* 4 10103 (1992).

evaluation of the result for the AC conductivity is given in the subsequent section, whereas the DC conductivity is discussed in section 5, emphasizing the Mott transition. The main part of the paper concludes with the discussion in section 6.

2. Model

2.1. Hamilton operator and formalism

We use a tight-binding Hamiltonian for spinless fermions with nearest-neighbour hopping, local disorder and nearest-neighbour repulsion (screened Coulomb interaction)

$$\hat{H} = \sum_i (\epsilon_i - \mu)\hat{n}_i + \sum_{i,j} t_{ij}\,\hat{c}_i^+ \hat{c}_j + \frac{1}{2}\sum_{i,j} U_{ij}\,\hat{n}_i\,\hat{n}_j \tag{1}$$

where $\hat{c}_i^+$ ($\hat{c}_i$) are the creation (annihilation) operators for the fermion on site i, $\hat{n}_i = \hat{c}_i^+ \hat{c}_i$ and $U_{ij}, t_{ij} = 0$ if i, j are not nearest neighbours. We shall investigate this Hamiltonian in the limit of high coordination number, $Z \to \infty$. For the model to remain non-trivial in this limit, the hopping matrix elements and the interaction matrix elements are scaled as $t_{ij} := -t/\sqrt{Z}$ and $U_{ij} := U/Z$, respectively [13, 23]. The energy ϵ_i is a stochastic variable drawn from some local site-independent distribution function $P(\epsilon)$. The chemical potential is μ. In what follows we will use the conventions $\hbar = 1$, $k_B = 1$ and $t = 1$†.

In order to calculate the conductivity we work with an extension of the Bethe lattice: the periodic Bethe lattice (PBL, see figure 1). It consists of linearly aligned and linked replicas of a simple Bethe lattice. Its coordination number Z is given by $K + 3$, where K is the branching ratio of the underlying Bethe lattice. The periodic Bethe lattice will be described more precisely in the subsequent section. At the present stage it is sufficient to state that it has the *same* one-particle properties as the underlying Bethe lattice in the limit under consideration, i.e. $Z \to \infty$.

In comparison with hypercubic lattices one easily sees that an important feature of a lattice in the correlation problem of spinless fermions, namely the bipartite structure, is shared by the Bethe lattice and the periodic Bethe lattice. Indeed, in the limit $Z \to \infty$ the PBL is *equivalent* to a hypercubic lattice with a half-elliptic DOS. This important equivalence is derived in appendix 2 for the thermodynamics and the conductivity. The half-elliptic DOS has realistic features in common with the true three-dimensional DOS: a finite band width and a square-root behaviour at the edges (contrary to the hypercubic infinite-dimensional Gaussian DOS found in [13]).

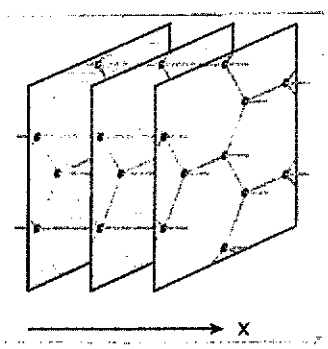

Figure 1. Part of the periodic Bethe lattice at $K = 2$; each sheet stands for one simple Bethe lattice. They are mutually connected to form a periodic structure in the x direction.

† In [VUV] it was erroneously stated that $t/\sqrt{K} = 1$, whereas it should be $t = 1$.

The Green function formalism we use is the locator formalism, which is the natural choice on a Bethe lattice [26]. Local operators constitute the unperturbed Hamiltonian; hopping and interactions induce a self-energy $\Sigma_{ij}(\omega)$.

It is here that the limit $Z \to \infty$ enters, essentially by suppressing certain classes of diagrams (for details see section 2.1 in [VUV]). To illustrate this point we state (i) that in the pure interacting case (no disorder), in the limit of infinite coordination number, only the Hartree diagrams survive [23], and (ii) that in the pure disorder case (no interaction) the coherent-potential approximation (CPA) becomes exact in the limit $Z \to \infty$ [24]. If both disorder and interaction are present the limit $Z \to \infty$ is still extremely useful: the self-energy is still local $\Sigma_{ij}(\omega) \to \Sigma_i(\omega)$ and it decouples into two independent contributions:

$$\Sigma_i(\omega) = \sigma_i(\omega) + s_i. \tag{2}$$

In the locator formalism $\sigma_i(\omega)$ results from the hopping and s_i from the interaction; they are straightforward to calculate, see equation (8) of [VUV]. (The site subscript distinguishes between the self-energy $\sigma_i(\omega)$ and the conductivity $\sigma(\omega)$.)

The locality of the self-energy is a typical mean-field property and is found in the limit of infinite coordination number for any form of interaction and disorder [11]. In general models, however, the decoupling is not complete: the two contributions in (2) depend on each other self-consistently and s_i is also ω dependent.

2.2. *Thermodynamic properties*

We would like to emphasize that all subsequent results are equally valid for hypercubic lattices in the limit $d \to \infty$ assuming a half-elliptic DOS, although hypercubic lattices contain loops in contrast to the Bethe lattice. Since we deal in any case with bipartite lattices, i.e. lattices of A–B structure, we have to take into account at least two phases depending on the interaction strength U: at low U the homogeneous phase (invariant under the discrete lattice translations), and at high U a checkerboard phase or charge-density wave (CDW) with alternating particle densities. The latter is the symmetry-broken phase in which two locators, g_L and g_U, can be distinguished. The locator g_L describes fermions on the sublattice with the higher particle density: these electrons have on average a lower energy (indicated by the subscript L, denoting 'low'). The locator g_U describes fermions on the sublattice with the lower particle density: these electrons have on average a higher energy (indicated by the subscript U, denoting 'up'). The appropriate order parameter is half the difference of the particle densities $b := \frac{1}{2}(n_L - n_U)$ or the ensuing energy difference $\Delta := Ub$.

In the following we choose to work with a semi-elliptic probability distribution $P(\epsilon) = (\pi\sqrt{\gamma})^{-1}\sqrt{1 - \epsilon^2/4\gamma}$ for the random site energies ϵ representing the disorder (equation (13) of [VUV]). Thereby $4\sqrt{\gamma}$ is the width of $P(\epsilon)$. The locators are then given by the equations (see equations (14) of [VUV]):

$$\gamma\, g_U{}^2 - (\omega - g_L - \Delta)\, g_U + 1 = 0 \tag{3a}$$

$$\gamma\, g_L{}^2 - (\omega - g_U + \Delta)\, g_L + 1 = 0. \tag{3b}$$

The order parameter and the chemical potential are determined by the self-consistent equations (see equation (15) of [VUV])

$$n(\beta, \gamma) = -\int_{-\infty}^{\infty} \frac{d\omega}{2\pi}\, \mathrm{Im}[g_L(\omega) + g_U(\omega)]\, f_F(\omega) \tag{4a}$$

$$U(\beta, \gamma) = -\Delta\left(\int_{-\infty}^{\infty} \frac{d\omega}{2\pi}\, \mathrm{Im}[g_L(\omega) - g_U(\omega)]\, f_F(\omega)\right)^{-1} \tag{4b}$$

where $f_F(\omega)$ is the Fermi distribution function. In figure 2 three generic results of (3) are shown. The global density of states is $\rho(\omega) = -(\mathrm{Im}g_L + \mathrm{Im}g_U)/2\pi$. For order parameters Δ larger than $\Delta_S = 2\gamma/\sqrt{1+\gamma}$, band splitting occurs. (Throughout the present paper the subscript S indicates the values where band splitting occurs. This slightly changes the notation compared to equation (19) of [VUV].) The value for Δ_S can be found by solving (3) at $\omega = 0$, since $\rho(-\omega) = \rho(\omega)$. For $\Delta > \Delta_S$ there is an energy gap in the DOS denoted by $2D$. For $\Delta < \Delta_S$ there are no inner band edges, but either a minimum or a maximum depending on Δ. From (3) the behaviour of $\rho(\omega)$ is found to be

$$\rho(\omega) - \rho(0) \propto \pm\omega^2 \qquad \Delta < \Delta_S \quad \text{for } \omega \approx 0 \tag{5a}$$

$$\rho(\omega) = \frac{\sqrt{3}}{2\pi[\gamma(1+\gamma)^2]^{1/3}}|\omega|^{1/3} \qquad \Delta = \Delta_S \quad \text{for } \omega \approx 0 \tag{5b}$$

$$\rho(\omega) \propto (|\omega| - D)^{1/2} \qquad \Delta > \Delta_S \quad \text{for } |\omega| \approx D. \tag{5c}$$

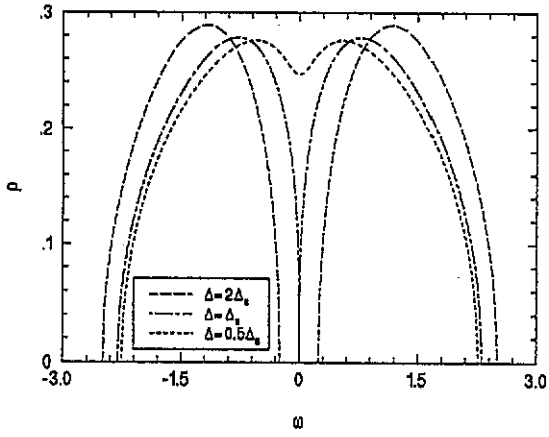

Figure 2. DOS at fixed disorder γ against the energy for various values of the order parameter Δ; band splitting occurs at Δ_S.

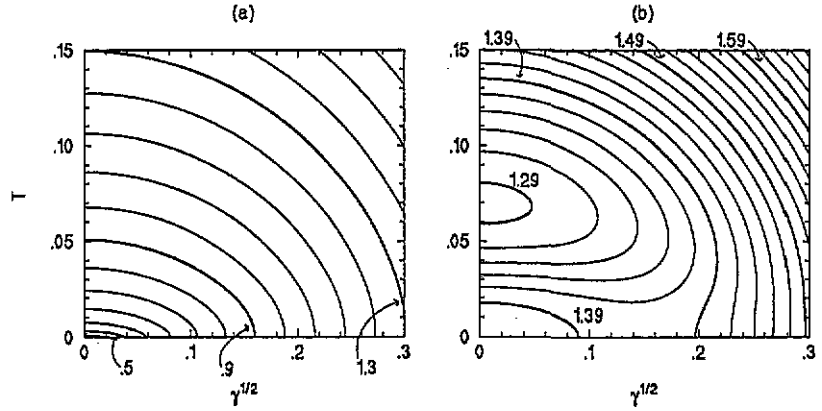

Figure 3. Contour plots displaying lines of constant critical interaction U_c in the T–$\sqrt{\gamma}$ plane: (*a*) $n = 0.5$; (*b*) $n = 0.45$.

The more detailed form for (5*b*) results from the possibility of solving (3) exactly for $\Delta = \Delta_S$ and expanding around that solution. The Green functions for small ω are

$$g_{L/U}(\omega) = \pm\frac{1}{\sqrt{1+\gamma}} - \frac{\mathrm{sgn}(\omega) + \mathrm{i}\sqrt{3}}{2[\gamma(1+\gamma)^2]^{1/3}}|\omega|^{1/3}. \tag{6}$$

One of the amazing features found in an attentive examination of the solutions of (4) is the anomalous behaviour of the symmetry breaking as a function of temperature T and disorder $\sqrt{\gamma}$. Away from half filling, temperature and/or disorder may even facilitate spontaneous symmetry breaking to a certain extent. There are parameter ranges in which finite values of the order parameter are only found at $T > 0$. This phenomenon can be understood as the consequence of particle-density fluctuations induced by finite T or γ. They bring the system in certain regions closer to half filling, where the tendency towards symmetry breaking is extremely high. For details we refer the reader to [VUV]. To provide nevertheless an overview of the anomaly we include a new and comprehensive figure: figure 3. The critical interaction U_c is the value above which the order parameter Δ is finite. Its value can be computed from (4) in the limit $\Delta \to 0$.

In figure 3 curves of constant U_c are plotted in the plane of T and $\sqrt{\gamma}$. (The square root is taken to have two quantities with the same dimension.) In figure 3(*a*) the scenario is shown at half filling. *No* anomaly can be seen; an increase of T or $\sqrt{\gamma}$ increases U_c. Moreover, a crossover behaviour can be conjectured, since the equipotential curves have an elliptic shape: U_c can be described by a function of a quadratic form of T and $\sqrt{\gamma}$. In figure 3(*b*) the corresponding curves at $n = 0.45$ are displayed. In comparison with half filling, three facts are remarkable: (i) the minimum of U_c is *not* at the origin (anomaly); (ii) there is *no* obvious, simple relation linking T and $\sqrt{\gamma}$; (iii) there is *no* symmetry $T \longleftrightarrow \sqrt{\gamma}$ which would give evidence that dynamic and static fluctuations have *quantitatively* the same effect. Qualitatively, however, they display a similar behaviour.

The contour plot gives a quantitative insight in the structure of the anomaly and its dependence on the disorder and the temperature. As such it is the most important finding of this section. The existence of the anomaly will also be visible in transport properties.

3. Transport

We now treat the problem of transport on the Bethe lattice. If a system is subject to an electrical field the electrons drift in the field direction, thereby giving rise to an electrical current. Necessary for a finite DC conductivity is elastic scattering by impurities, which destroys the initial momentum of the electrons. On the Bethe lattice, however, there is no translational invariance to define a momentum. Therefore, although it is possible to discuss concepts like localization [27], ballistic and diffusive transport are indistinguishable.

The problem set out above can be circumvented by extending the lattice in such a way that it allows a momentum definition in at least one direction. We therefore choose a lattice which is periodic in one spatial direction, say x, and is of the Bethe kind perpendicular to x, see figure 1. Impurities may scatter electrons with momentum p_x to another momentum p'_x. Hopping in the x direction is also scaled with $1/\sqrt{K}$. This implies that the thermodynamics is that of the Bethe lattice, since the sheets effectively decouple at the one-particle level.

We stress that *all* results obtained on the periodic Bethe lattice are equal to results achieved on a hypercubical lattice with infinite dimensions, where the Gaussian DOS is replaced by a semi-elliptic DOS. The latter is, of course, exactly the DOS of the Bethe lattice with infinite coordination number. Thus we see that the lattice structure *only* enters via the DOS of the free-electron problem (for details see appendix 2).

The conductivity is found from

$$\sigma(\omega) = -e^2 \frac{i\omega}{2} \sum_{r,x} x^2 N(r) \chi^{\rho\rho}(x, r; \omega) \tag{7}$$

where $N(r) = (K+1)K^{r-1}$, $r \geqslant 1$, counts the number of sites on a shell at distance r on the Bethe lattice. The distance in the periodic direction is given by x, which takes integer values. The lattice constant is set to unity. The term $\chi^{\rho\rho}(x, r; \omega)$ is the density–density response function:

$$\chi^{\rho\rho}(x, r; \omega) := -i \int_0^\infty dt \exp(i(\omega + i0^+)t) \langle [\hat{n}(x, r; t), \hat{n}(0, 0; 0)] \rangle. \tag{8}$$

From the scaling of the hopping we know that $\chi^{\rho\rho}(x, r; w) \propto K^{-x}$ in the limit $K \to \infty$. Since the term with $x = 0$ does not contribute in (7) the leading order of $\sigma(\omega)$ is $1/K$. Thus we have to calculate $\chi^{\rho\rho}(1, r; \omega)$. This implies that in the limit $K \to \infty$ only two sheets of the periodic structure are important. Clearly it is the interplane hopping (i.e. hopping between the two sheets) from which the $1/K$ dependence originates.

The interplane density–density response function $\chi^{\rho\rho}(r, \omega) := \chi^{\rho\rho}(1, r; \omega)$ is directly connected to the interplane two-particle propagator. We look for an expression for $\sum_r N(r)\chi^{\rho\rho}(r, w)$ in terms of Green functions.

The intraplane diagrammatic elements $G^{(2)}$ are taken from equation (4) of [VUV]. The general interplane two-particle Green function $H^{(2)}$ is given by

$$\begin{aligned} H^{(2)}_{ijhk}(z_l, z_m, z_n) = \beta^{-1} \sum_p \sum_{f,f',g,g'} G^{(2)}_{g',j,h,f'}(z_l, z_p, z_n) t_{g,g'} t_{f,f'} G^{(2)}_{i,f,g,k}(z_l + z_p - z_n, z_m, z_p) \\ + \beta^{-2} \sum_{p,q} \sum_{f,f'} G^{(2)}_{f',j,h,f'}(z_l, z_p, z_n) U_{f,f'} G^{(2)}_{i,f,f,k}(z_q + z_l - z_n, z_m, z_q) \end{aligned} \tag{9}$$

where the hopping and interaction are interplane. The calculation is simplified considerably since the diagrammatic contribution $B(z_l)$ for $\sigma(\omega)$ that consist of one or more 'bubbles' vanishes

$$B(z_l) = \beta^{-1} \sum_m \sum_r G^{(2)}(r; z_m, z_m - z_l) = 0. \tag{10}$$

This applies equally as well to the second term in (9) (interplane) as to an internal explicit dependence of U in $G^{(2)}$ (intraplane). Thus the interaction *only* enters the calculation through one-particle Green functions and $H^{(2)}$ depends on two frequencies. We define

$$H^{(2)}(z_l, z_m) := \frac{1}{2\beta} \sum_n \sum_j \prod_k \int d\epsilon_k P(\epsilon_k) \left(H^{(2)}_{ijji}(z_l, z_m, z_n)\Big|_{i \in U} + H^{(2)}_{ijji}(z_l, z_m, z_n)\Big|_{i \in L} \right). \tag{11}$$

This expression sums over all r, $\sum_r N(r)$, and averages over the two sublattices. The conductivity may now be expressed as

$$\sigma(\omega) = e^2 \frac{z_m}{\beta} \sum_l H^{(2)}(z_l, z_l - z_m)\Big|_{z_m \to i(\omega + i0^+)} \tag{12}$$

where $z_m \to \mathrm{i}(\omega + \mathrm{i}0^+)$ denotes the analytical continuation of the Matsubara frequencies. In appendix 1 an explicit expression for $H^{(2)}(z_l, z_m)$ is derived:

$$H^{(2)}(z_l, z_m) = \frac{K^{-1}}{(z_l - z_m)^2}\left(\frac{g_U(z_l)g_L(z_l)}{1 - g_U(z_l)g_L(z_l)} + \frac{g_U(z_m)g_L(z_m)}{1 - g_U(z_m)g_L(z_m)} - \frac{2 + g_U(z_l)g_L(z_m) + g_U(z_m)g_L(z_l)}{1 - g_U(z_l)g_U(z_m)g_L(z_l)g_L(z_m)} + 2\right). \tag{13}$$

Apart from contributions proportional to $\delta(\omega)$ we obtain for the real part of the conductivity from (12) and (13)

$$\mathrm{Re}\sigma(\omega) = -\frac{e^2}{K\beta z_m} \times \sum_l \left(\frac{2 + g_U(z_l)g_L(z_l - z_m) + g_L(z_l)g_U(z_l - z_m)}{1 - g_U(z_l)g_U(z_l - z_m)g_L(z_l)g_L(z_l - z_m)} - 2\right)\Bigg|_{z_m \to \mathrm{i}(\omega + \mathrm{i}0^+)}. \tag{14}$$

In this expression only one-particle Green functions appear. Hence, there are no vertex corrections for this model in the limit $K \to \infty$. This can be seen even more explicitly in the equivalent derivation for the hypercubic case in appendix 2. In appendix 3 it is proven that the f-sum rule for the conductivity is fulfilled.

4. AC conductivity

4.1. Homogeneous state

As stated in [VUV] (section 3 (ii)), a finite interaction does not change g_U and g_L as long as the system remains in the homogeneous phase. This can be seen directly from (3), where only Δ appears. Using (14) at $\Delta = 0$ the conductivity becomes

$$\mathrm{Re}\sigma(\omega) = \frac{2e^2}{\pi K} \int_{\omega/2 - 2\sqrt{\gamma+1}}^{-\omega/2 + 2\sqrt{\gamma+1}} \mathrm{d}x \frac{f_F(x - \omega/2) - f_F(x + \omega/2)}{\omega} \times \frac{\gamma(\gamma+2)}{(\gamma+2)^2(4\gamma^2 + \omega^2) - (2\gamma x)^2}[4(\gamma+1) - (x + \omega/2)^2]^{1/2} \times [4(\gamma+1) - (x - \omega/2)^2]^{1/2}. \tag{15}$$

In figure 4(*a*) this result is plotted for various values of the temperature and the disorder away from half filling. The result is a typical CPA result; for a review on CPA see [28]. What is essentially observed is a broadening, proportional to $\sqrt{\gamma}$, of the Drude peak at $\omega = 0$ and a $1/\omega^2$ decay for intermediate ω.

4.2. CDW without disorder

In the case of zero disorder and a large enough interaction to drive the system into a CDW (i.e. $\Delta > 0$) the conductivity becomes

$$\mathrm{Re}\sigma(\omega) = -\frac{e^2}{K}\Bigg[\delta(\omega) \int_{\Delta}^{\sqrt{\Delta^2+4}} \frac{\mathrm{d}x}{x}[(\Delta^2 + 4 - x^2)(x^2 - \Delta^2)]^{1/2}\left(\frac{\partial f_F}{\partial x}(x) + \frac{\partial f_F}{\partial x}(-x)\right) + \frac{\Delta^2}{\omega^2}\left(\frac{4\Delta^2 + 16 - \omega^2}{\omega^2 - 4\Delta^2}\right)^{1/2}[f_F(\omega/2) - f_F(-\omega/2)]\mathrm{sgn}(\omega)\Bigg] \tag{16}$$

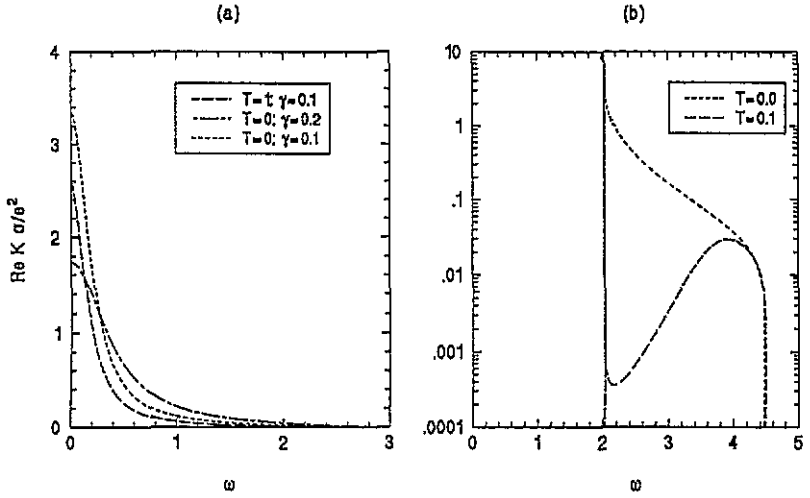

Figure 4. The real part of the dynamical conductivity $\sigma(\omega)$ at $n = 0.45$ for two special cases: (*a*) $\Delta = 0$ (homogeneous phase) and finite γ; (*b*) $\gamma = 0$ and finite Δ (CDW) at $U = 3$. The Drude δ-peaks at $\omega = 0$ in (*b*) are not shown.

where ω takes only values such that the square roots are real; otherwise $\sigma(\omega)$ equals zero. For various values of the interaction and temperature the conductivity is plotted in figure 4(*b*) (the Drude peak is not shown). For finite ω we observe a real contribution resulting from resonances between the subbands. For zero temperature there is a divergence at frequencies equal to the band gap and a monotonic decrease. For finite temperatures the divergence remains and a minimum appears due to the minimum in the product of the DOS and the Fermi distribution away from half filling.

4.3. Finite disorder and interaction at half filling

For $\sigma(\omega)$ a simple expression cannot be given for finite disorder in the CDW phase. We have to extract g_U and g_L from (3) and insert them in (14). The necessary μ and Δ values are self-consistently determined using (4).

In figure 5(*a*) the conductivity is plotted for various values of the disorder at zero temperature. In our example we have a gap in the conductivity at $\gamma < \gamma_s = 0.25$, where γ_s is related to the order parameter at which splitting occurs by $\Delta_s = 2\gamma_s/\sqrt{\gamma_s + 1}$. Since the conductivity vanishes at $\omega = 0$ the system is in the Mott insulating state. For $\gamma < \gamma_s$ the disorder is *not* large enough to close the gap in the DOS. At the value $\omega = 2D$, where the gap in the conductivity ends, we have a quadratic behaviour $\sigma(\omega) \propto (\omega - 2D)^2$. In the case $\gamma = \gamma_s$ the gap in the DOS is marginal, and so is the gap in the conductivity. This is the Mott transition point. After some algebra using (14) and (5*b*) one finds at this point

$$\mathrm{Re}\sigma(\omega) = \frac{e^2}{2\pi K}\frac{3}{(\gamma_s + 2)\Delta_s}\left(\frac{4}{\gamma_s \Delta_s}\right)^{1/3}|\omega|^{2/3} \tag{17}$$

for small ω. For larger disorder we see that the gap is closed by the broadening of the subbands so that we have a finite conductivity at $\omega = 0$. Due to the symmetry $\mathrm{Re}\sigma(-\omega) = \mathrm{Re}\sigma(\omega)$ we have a quadratic extremum at $\omega = 0$.

For a fixed value of the disorder, $\mathrm{Re}\sigma(\omega)$ is depicted in figure 5(*c*) at various temperatures. For zero temperature the gap is visible, but for an arbitrarily small temperature

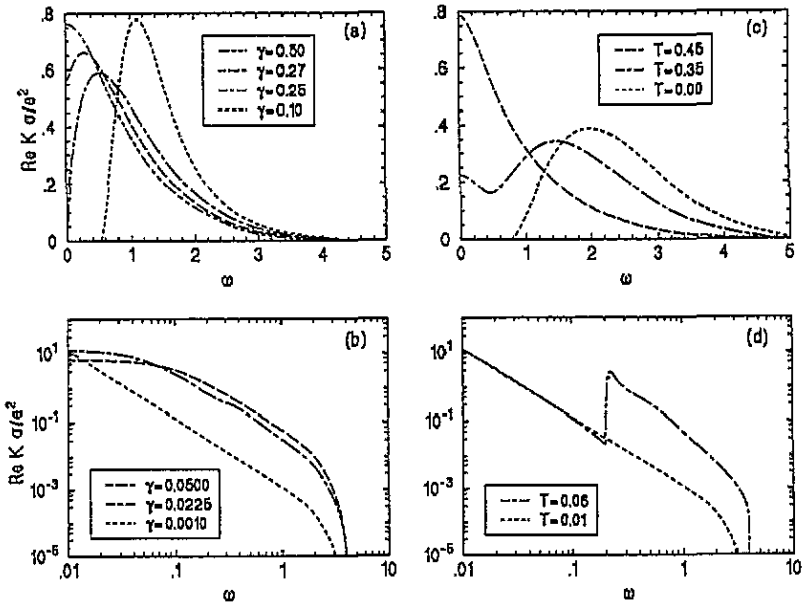

Figure 5. $\mathrm{Re}\sigma(\omega)$ in four generic cases: (*a*) $T = 0$, $n = 0.50$, $U = U_S|_{\gamma=0.25}$; (*b*) $T = 0$, $n = 0.45$, $U = 1.39$; (*c*) $\gamma = 0.25$, $n = 0.50$, $U = 2.80$; (*d*) $\gamma = 0.001$, $n = 0.45$, $U = 1.39$. Plots (*a*) and (*c*) display the gap in the conductivity; (*b*) and (*d*) display the effect of the anomaly.

it is smeared out. As a result, a thermally induced finite DC conductivity appears and a minimum at finite frequencies. For larger temperatures the systems enters the homogeneous phase again.

4.4. Finite disorder and interaction away from half filling

Figure 5(*b*) depicts three curves at different values of disorder to show the effect of the anomaly. The system is in the homogeneous state for the highest and lowest disorder, but in the CDW for the intermediate. The anomaly manifests itself through the small wiggle at $\mathrm{Re}\omega \approx 0.3$.

The anomaly is much more visible in the temperature dependence of $\mathrm{Re}\sigma(\omega)$. Figure 5(*d*) gives $\mathrm{Re}\sigma(\omega)$ for two temperatures. The real part of the conductivity shows an increase of two orders of magnitude at $\omega \approx 0.2$ when the temperature is increased so that the system enters the CDW phase. For even higher temperatures the system turns homogeneous again, and the conductivity nearly equals that at low temperatures (not displayed).

In figure 6(*a*) the real part of the conductivity is depicted as a function of frequency and temperature at half filling. The Mott gap is clearly visible. For higher temperatures the minimum at $\omega = 0$ disappears and for $T > 0.27$ the system is in the homogeneous phase with a quadratic maximum in $\mathrm{Re}\sigma$ at $\omega = 0$. Note that for temperatures just below the critical temperature, $T_c \approx 0.27$, there exists a pronounced central peak, which can also be recognized in figure 5(*c*). It is due to thermal excitations. In figure 6(*b*) $\mathrm{Re}\sigma(\omega, T)$ is depicted away from half filling, $n = 0.45$. Since the Fermi level is always in a region where the DOS is finite the DC conductivity is never zero. This expresses itself by the existence of the *additional* central peak around $\omega = 0$ *even* at zero temperature.

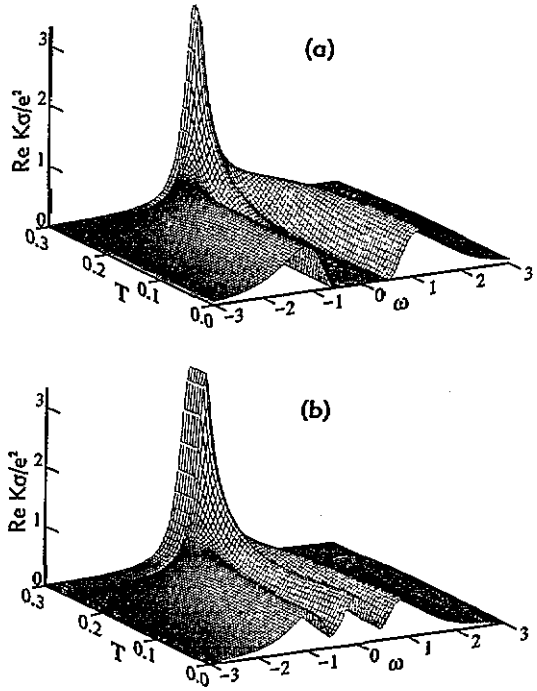

Figure 6. Reσ against the frequency ω and the temperature T at $U = 2$ and $\gamma = 0.1$: (*a*) $n = 0.5$; (*b*) $n = 0.45$.

5. DC conductivity

5.1. Effect of the anomaly

Resulting from (13) or (A1.12) and (12) we have for zero temperature

$$\sigma_{DC} = \frac{2\pi e^2}{K} \frac{(\rho_U + \rho_L|g_U|^2)(\rho_L + \rho_U|g_L|^2)}{(1 - |g_L|^2|g_U|^2)|1 - g_U g_L|^2}\bigg|_{\omega=\mu}. \tag{18}$$

To include finite temperatures it suffices to convolute $\sigma_{DC}(\mu)$, as given above, with the temperature peak $\frac{\partial}{\partial\mu} f_F$.

Figure 7 shows solutions of (18) and (4) for finite dopings. The curve for $n = 0.495$, corresponding to very low doping, displays the conventional and expected behaviour: increasing temperature induces a decrease of the order parameter Δ leading to a higher DC conductivity. Once the spontaneous ordering has been suppressed completely σ_{DC} depends only very little on the temperature ($T > 0.15$). The curve for higher doping $n = 0.45$, instead, shows anomalous behaviour: there is *no* spontaneous ordering at low temperatures $T < 0.022$, but a *finite* Δ occurs in an intermediate range of T. This increase of Δ induces an unexpected dip in the DC conductivity. Hence, the thermodynamic anomaly away from half filling also induces an anomalous effect in the transport property σ_{DC}.

5.2. Mott transition

We now turn to the investigation of the Mott transition at half filling. For a sufficiently large interaction, band splitting occurs for $\Delta \geqslant \Delta_S$ so that the DC conductivity σ_{DC} vanishes at $n = 0.5$ and $T = 0$. It is of interest to know how the DC conductivity σ_{DC} disappears, depending on one of the possible parameters: interaction U, disorder γ, doping $\delta = 1/2 - n$, temperature T and frequency ω.

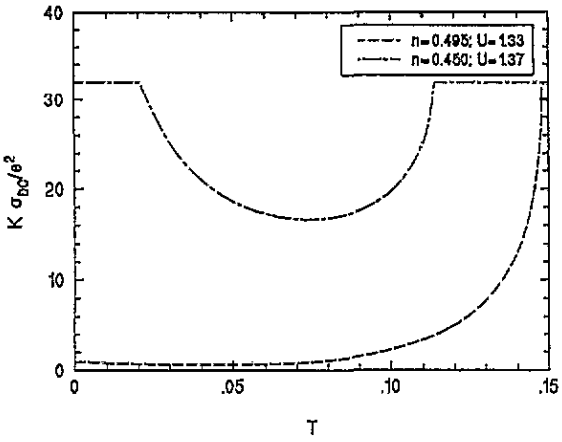

Figure 7. DC conductivity against T for different dopings and interactions at fixed $\gamma = 0.1$. The curve at higher doping shows the generic effect of the anomaly, the curve at lower doping the conventional behaviour.

For $\omega = \mu = 0$ we obtain from (3) the retarded Green functions g_L and g_U:

$$g_L = \Delta/(2\gamma) - i[1/(1+\gamma) - \Delta^2/4\gamma^2]^{1/2} \tag{19a}$$

$$g_U = -\Delta/(2\gamma) - i[1/(1+\gamma) - \Delta^2/4\gamma^2]^{1/2}. \tag{19b}$$

Inserting this in (18) yields

$$\sigma_{DC} = \frac{2e^2}{\pi K}\frac{(1+\gamma)}{\gamma(2+\gamma)}\left(1 - \Delta^2\frac{1+\gamma}{4\gamma^2}\right) \tag{20}$$

which implies a vanishing DC conductivity for values of the order parameter Δ greater than $2\gamma/\sqrt{1+\gamma}$. This was to be expected since this is the value Δ_S where band splitting occurs. In figure 8 the DC conductivity is given as a function of the interaction U and the disorder parameter γ, respectively. These curves result from (20) and (4). To find the dependence of σ_{DC} on the filling n and the temperature T one has to go back to (18) including the subsequent remark for finite temperatures, figure 9.

The onset of the conductivity in figures 8 and 9 is described by the power law characterized by a critical exponent or by the exponential behaviour with which σ_{DC} rises.

(i) Concerning the dependence on the interaction U and the disorder γ it can easily be seen that this power law is a *linear* one: at $\Delta \neq 0$, Δ depends differentially on U and γ so that the vanishing of σ_{DC} in (20) is governed by a factor $U_S - U$ or $\gamma - \gamma_S$, respectively. Thus the critical exponent of interaction and disorder is one, which can easily be recognized in figure 8.

The other interesting singularity in figure 8 is the cusp in σ_{DC} due to the onset of the symmetry breaking. For small order parameter Δ, the lowering of σ_{DC} is proportional to Δ^2, which in return depends linearly on $U - U_c$ or $\gamma_c - \gamma$ respectively. Hence the cusp is linear on both sides. The same cusp is found for the dependence on doping and temperature in figure 9.

(ii) In a discussion of the critical exponents of the doping, temperature and frequency, it is necessary to distinguish whether the order parameter Δ_0 at $T = 0$ and $n = 1/2$ is greater than, equal to or lower than Δ_S. The results for the ω dependence have already been given in section 4. For the other dependencies we learn from (18) that $\sigma_{DC}(\mu)$ is proportional

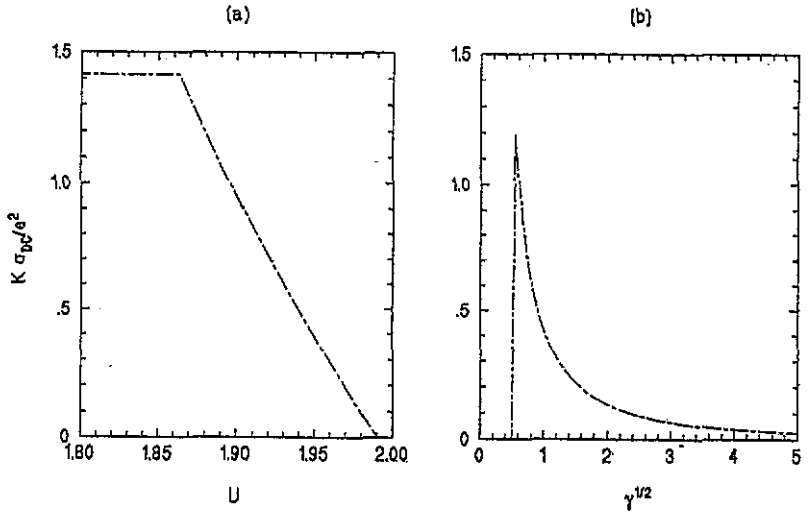

Figure 8. DC conductivity at $n = 0.5$ and $T = 0$: (*a*) against U at $\gamma = 0.25$; (*b*) against $\sqrt{\gamma}$ at $U = U_S|_{\gamma=0.25}$.

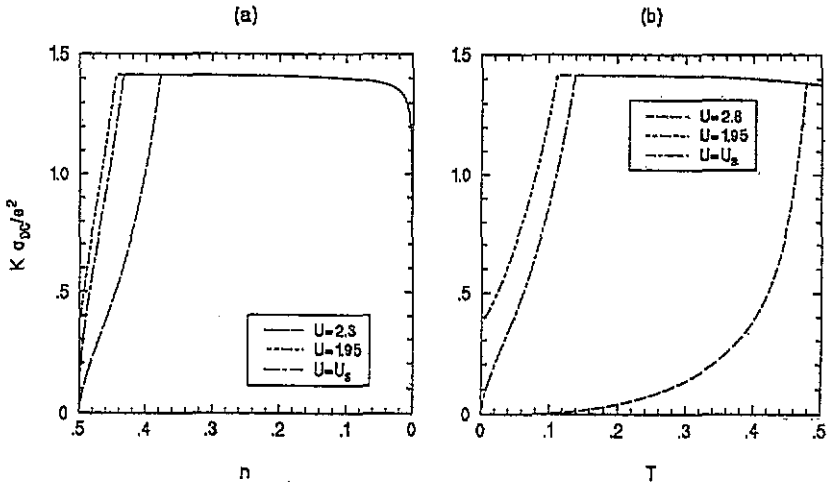

Figure 9. DC conductivity at fixed $\gamma = 0.25$ for different interactions corresponding to the three generic cases in the relation of Δ_0 to Δ_S: (*a*) σ_{DC} against n at zero temperature; (*b*) σ_{DC} against T at half filling.

to $\rho^2(\mu)$ or to the convolution of $\rho^2(\mu)$ with the temperature peak at $T \neq 0$. (It is not necessary to distinguish between ρ_U and ρ_L at the present stage since we are only interested in the critical onset.) We refer to (5) for the results for $\rho(\mu)$.

For $\Delta_0 < \Delta_S$ the conductivity σ_{DC} does not vanish since no complete band splitting occurs. Instead it displays a quadratic minimum. To see that this statement is correct, not only for δ but also for T, we verified that the direct decrease of $\Delta(T)$ is quadratic, too, i.e. $(\Delta(T) - \Delta_0) \propto -T^2$, at half filling, which is important in the analysis of (20).

In the marginal case $\Delta_0 = \Delta_S$ the band edge is given by a cubic-root dependence, see (5*b*). This induces $\sigma_{DC} \propto \delta^{1/2}$ and $\sigma_{DC} \propto T^{2/3}$. Note that in the calculation of the

dependence on doping, the DOS $\rho(\mu)$ also enters via $\delta = \int \rho(\mu)\mathrm{d}\mu$, see (4*a*). In addition to the simple power laws we may also compute the coefficients, since we know the form of the Green functions more precisely in the marginal case (6). Using (18) yields in leading order

$$\sigma_{\mathrm{DC}}(\delta) = \frac{e^2}{K}\left(\frac{2\sqrt{3}}{\pi}\right)^{1/2}\frac{1+\gamma}{\gamma^{3/2}(2+\gamma)}\sqrt{\delta} \tag{21a}$$

$$\sigma_{\mathrm{DC}}(T) = \frac{e^2}{K}\frac{2(1-2^{1/3})}{\pi}\Gamma(2/3)\zeta(2/3)\frac{(1+\gamma)^{2/3}}{\gamma^{5/3}(2+\gamma)}T^{2/3} \tag{21b}$$

where $\Gamma(x)$ and $\zeta(x)$ are the Gamma function and the Riemann zeta function, respectively.

In the general case $\Delta_0 > \Delta_S$ the band edge is characterized by a quadratic root, see (5*c*). This leads to a critical exponent 2/3 in the δ dependence of σ_{DC}. The temperature dependence is no longer given by a power law since a real band gap $D_0 > 0$ is present. Note that D_0 and Δ_0 are identical only for vanishing disorder $\gamma = 0$. In general D_0 is smaller than Δ_0 and becomes zero for $\Delta_0 = \Delta_S$. Due to D_0 and the behaviour of the band edges σ_{DC} is proportional to $T\exp(-D_0/T)$ at low temperatures.

The results for the δ and T dependence of the DC conductivity are summarized in table 1.

Table 1.

Variable	δ	T	ω
$\Delta_0 < \Delta_S$	2	2	2
$\Delta_0 = \Delta_S$	$\frac{1}{2}$	$\frac{2}{3}$	$\frac{2}{3}$
$\Delta_0 > \Delta_S$	$\frac{2}{3}$	∞	2

The exponents provide a complete characterization of the Mott transition in the system under investigation. It is remarkable that the critical exponents differ in different parameter ranges and depend on the variable, i.e. interaction U, disorder γ, doping δ, temperature T and frequency ω. This leads to the important conclusion that *no* general crossover is given: even variables of the same dimension entail different critical dependencies.

Another interesting feature is found in figure 9(*a*) in the range of filling where the order parameter Δ is zero (the homogeneous phase). The DC conductivity has a box-like dependence on the filling: σ_{DC} is nearly independent on n until n is very close to the empty band. This can be understood by writing down (15) for $\omega = 0$

$$\sigma_{\mathrm{DC}}(\mu) = \frac{e^2}{2\pi K}\frac{2+\gamma}{\gamma}\left(1 - \frac{\gamma^2}{(2+\gamma)^2 - \mu^2}\right). \tag{22}$$

The DC conductivity depends only weakly on the chemical potential. Its dependence on the temperature is also fairly weak since the convolution of an almost constant function again yields an almost constant function.

6. Discussion

In the present paper we have discussed and extended the exact solution [VUV] of a model of spinless fermions with a nearest-neighbour interaction and local disorder in the limit of infinite coordination number. The essential thermodynamic properties are recalled, especially the anomalously facilitated symmetry breaking by weak fluctuations due to temperature or disorder.

We introduced and calculated the conductivity using our previously established thermodynamic results. We extended the simple Bethe lattice to the periodic Bethe lattice, PBL, consisting of linearly arranged and linked parallel sheets of Bethe lattices. This allowed us to define a (crystal) momentum in the direction of periodicity. Disorder scatters states of well defined momentum, thereby inducing diffusion in contrast to ballistic propagation. In addition to the introduction of the conductivity on the PBL we derived the explicit expression for it in the limit $Z \to \infty$. We proved thereby that the limit of high coordination number not only allows one to deal with interaction and disorder on an equal footing in the one-particle properties, but also in the two-particle properties. It turned out that the limit $Z \to \infty$ suppresses all vertex corrections and preserves the f-sum rule linking $\int d\omega \sigma(\omega)$ to the kinetic energy.

Moreover, we applied the limit of high coordination number to hypercubic lattices and showed that the basic equations for this problem are the same as for the Bethe lattice. The use of the same unperturbed DOS leads to identical equations. Although this fact was expected for the thermodynamics its verification provides further insight into the essential ingredients: the limit $Z \to \infty$ and the bipartite structure. We proved under the same preconditions that this equivalence can be extended to the dynamical conductivity. This is an interesting and less obvious finding which, extends our knowledge of the general properties of the limit of high coordination number.

Subsequently, we discussed in great detail the effects of the phase transition on the conductivity, emphasizing two phenomena: (i) the effects of the anomalous behaviour in the AC and DC conductivity, and (ii) the Mott transition at half filling and zero temperature due to the band splitting.

We found that a finite order parameter leads to gap structure in the AC conductivity and to a lowering of the DC conductivity. Away from half filling these effects occur in a certain parameter range on increasing temperature and/or disorder. This is the signature of the anomalous behaviour.

The DC conductivity vanishes at half filling and zero temperature for a strong enough interaction. This is the so-called Mott transition. It is characterized by the behaviour of σ_{DC} when the parameters approach their critical values. We calculated the critical exponents for doping, temperature, interaction, disorder and frequency. They depend in general on the parameter range and the considered variable. No general crossover can be observed.

It is not easy to make contact between experimental data and our results since, to our knowledge, experiments have focused on systems containing spin degrees of freedom. Yet there exist real systems, such as magnetite, which are described by a model of spinless fermions. However, magnetite has an inverse spinel structure and is thus not bipartite. Furthermore, a realistic description of the material requires polaronic effects [29], which explains that the Verwey transition is of first order. Nevertheless, our findings agree qualitatively with the temperature dependence of the DC conductivity below the Verwey transition, which is dominated by the existence of a gap and the fact that the order parameter does not attain its possible maximal value 0.5 [30]. Quantitatively, however, we find in our model that the ratio D_0/T_c is bound from above by 2, whereas it takes the value ≈ 6 in magnetite.

The lack of reference data also extends to quantum Monte Carlo simulations, since Hubbard-like models have attracted much more attention. We propose to investigate more closely spinless fermion systems, both by experiment and by simulation, in order to obtain a thorough understanding of the metal–insulator transition (MIT), where this important transition is not obscured by transitions involving the spin degrees of freedom [7–9]. A complete understanding of the MIT in the simpler spinless fermion systems is a prerequisite

for a description of the MIT in the more complex situation with spin. This is particularly evident in the case where a separation of charge and spin degrees of freedom occurs [31,32], since the charge degrees of freedom carry the current.

Furthermore, a technical similarity between models with and without spin exists in infinite dimensions. The conductivity in the Hubbard model is given by the simple dressed bubble [25], as is the case in our model. No vertex corrections need to be included. *Thus similar densities of states lead to similar conductivities, as can be seen comparing* our findings with recent theoretical results for the Hubbard model in $d \to \infty$ [5, 15–18], which are supported by experimental data (see e.g. [33]). For a comparison of one-particle properties between spinless fermions and the results for the Hubbard model we refer the reader to [VUV].

The results presented in this paper, together with our findings in [VUV], prove the applicability of the limit of high coordination number as a systematic method of dealing with different perturbations on an equal footing. One-particle as well as two-particle properties can be dealt with. It is a systematic method since it is controlled by a small expansion parameter: the inverse coordination number $1/Z$. This leads naturally to possible further steps. Our results can be extended by including systematic $1/Z$ corrections, thereby accessing the region of finite dimensions. As a first step in this direction one should redo our calculations with the appropriate densities of states in finite dimensions. In variational treatments there are indications that this procedure yields very reasonable results, in agreement with Monte Carlo data [34].

Acknowledgments

We like to thank Professor D Vollhardt, Dr V Janiš and Dipl. Phys. R Strack for helpful discussions. The present work was partly supported by the SFB 341 of the Deutsche Forschungsgemeinschaft. One of us (GU) gratefully acknowledges the Studienstiftung des Deutschen Volkes for financial support.

Appendix 1.

In this appendix we calculate the general interplane two-particle propagator necessary to compute the dynamical conductivity. All properties are calculated in the symmetry-broken state, since the properties of the homogeneous state are simply deduced from this by putting the order parameter equal to zero.

A1.1. One-particle Green functions

The full locator, g_{U}, is given by

$$g_{\mathrm{U}}(z_l) = \int \mathrm{d}\epsilon_i P(\epsilon_i) g_i(z_l) = \int \mathrm{d}\epsilon_i P(\epsilon_i) \frac{g_i^0(z_l)}{1 - g_i^0(z_l)\left(\sigma_{\mathrm{U}}(z_l) + s_{\mathrm{U}}\right)} \tag{A1.1}$$

when $i \in \mathrm{U}$ and vice versa for $g_{\mathrm{L}}(z_l)$ with $i \in \mathrm{L}$ (see also equation (10) in [VUV]). The intraplane one-particle propagator $G(r; z_l)$ can be expressed as a power of these locators in the limit $K \to \infty$. This is because in the latter limit the self-energy is a local quantity, so that the propagator equals the free propagator with the energy shifted by Σ_i. The fact that we have two different self-energies for the different sublattices does not alter this. We

must distinguish between four situations, depending on whether i and j are members of the sublattice U or L. The propagator $G(r; z_l)$ is given by a 2×2 matrix:

$$G(r; z_l) = \prod_k \int d\epsilon_k P(\epsilon_k) G_{ij}(z_l)$$
$$= \begin{pmatrix} e(r) g_U(z_l) & o(r)[g_U(z_l) g_L(z_l)]^{1/2} \\ o(r)[g_L(z_l) g_U(z_l)]^{1/2} & e(r) g_L(z_l) \end{pmatrix} \left(\frac{g_L(z_l) g_U(z_l)}{K} \right)^{r/2} \tag{A1.2}$$

where $r = |i - j|$. For $r \geqslant 0$ we have $e(r) = [1 + (-1)^r]/2$ and $o(r) = [1 - (-1)^r]/2$, whereas for $r < 0$ we have $e(r) = o(r) = 0$. The elements in the first row describe propagation from sublattice U to sublattice U for r even, and to sublattice L for r odd. Similarly, the elements in the second row describe propagation starting from sublattice L. The diagonal part of $G(r, z_l)$, i.e. $G(0, z_l)$, is a 'matrix locator'.

We now turn to the interplane propagation on the PBL. One changes the sublattice as one propagates from one Bethe sheet to the next at equal Bethe coordinate. Therefore the direct hopping between the two Bethe sheets is

$$H_0 = -\frac{1}{\sqrt{K}} \begin{pmatrix} 0 & 1 \\ 1 & 0 \end{pmatrix}. \tag{A1.3}$$

On the PBL we calculate the interplane one-particle propagators in leading order of $1/K$. The term $H(0; z_l)$ describes the full propagation from one Bethe sheet to the other remaining at the same Bethe coordinate, whereas $\tilde{H}(r; z_l)$ describes propagation from a site on the first Bethe lattice to a site at distance r on the other lattice with the interplane hopping at a fixed intermediate site. The former is given by

$$H(0; z_l) = \sum_{s=0}^{\infty} N(s) G(s; z_l) H_0 G(s; z_l) = -\frac{1}{\sqrt{K}} \frac{g_L(z_l) g_U(z_l)}{1 - g_L(z_l) g_U(z_l)} \begin{pmatrix} 0 & 1 \\ 1 & 0 \end{pmatrix}. \tag{A1.4}$$

The two propagators $G(s; z_l)$ in (A1.4) describe the propagation on each Bethe sheet, and H_0 takes account of the interplane hopping. The sum counts all possible intermediate paths. The interplane propagator $\tilde{H}$ is basically the direct propagation with dressed hopping from one Bethe sheet to the other at a fixed intermediate site s. Thus we have

$$\tilde{H}(r; z_l) = G(s; z_l) G^{-1}(0, z_l) H(0; z_l) G^{-1}(0; z_l) G(r - s, z_l). \tag{A1.5}$$

Due to cancellation, $\tilde{H}$ is not dependent on s. Overcounting of locators in the product in (A1.5) is prevented by insertion of the inverse matrix locators $G^{-1}(0; z_l)$. Calculation yields

$$\tilde{H}(r; z_l) = \begin{pmatrix} o(r)[g_U(z_l)/g_L(z_l)]^{1/2} & e(r) \\ e(r) & o(r)[g_L(z_l)/g_U(z_l)]^{1/2} \end{pmatrix} \frac{(g_L(z_l) g_U(z_l)/K)^{(1+r)/2}}{1 - g_L(z_l) g_U(z_l)}. \tag{A1.6}$$

Note that the full interplane one-particle propagator $H(r; z_l)$, which is not needed in the present context, is given by $H(r; z_l) = \sum_{s=0}^{r} \tilde{H}(r; z_l) = (r + 1)\tilde{H}(r; z_l)$.

A1.2. Two-particle Green functions

The two-particle properties can be written down in terms of full one-particle Green functions and pure hopping. Remember that the U dependence only enters through these one-particle quantities. The locator is defined as

$$g_{\mathrm{U}}^{(2)}(z_l, z_m) = \prod_k \int \mathrm{d}\epsilon_k P(\epsilon_k) g_l(z_l) g_l(z_m) = \frac{g_{\mathrm{U}}(z_l) - g_{\mathrm{U}}(z_m)}{g_{\mathrm{L}}(z_l) - g_{\mathrm{L}}(z_m) + z_l - z_m} \tag{A1.7}$$

where the latter result is obtained using (A1.7). Just as in the one-particle situation, we have for the intraplane propagator

$$G^{(2)}(r; z_l, z_m) = \prod_k \int \mathrm{d}\epsilon_k P(\epsilon_k) G_{ijji}(z_l, z_m) = \left(\frac{g_{\mathrm{U}}^{(2)}(z_l, z_m) g_{\mathrm{L}}^{(2)}(z_l, z_m)}{K^2} \right)^{r/2} \times \begin{pmatrix} e(r) g_{\mathrm{U}}^{(2)}(z_l, z_m) & o(r)\sqrt{g_{\mathrm{U}}^{(2)}(z_l, z_m) g_{\mathrm{L}}^{(2)}(z_l, z_m)} \\ o(r)\sqrt{g_{\mathrm{L}}^{(2)}(z_l, z_m) g_{\mathrm{U}}^{(2)}(z_l, z_m)} & e(r) g_{\mathrm{L}}^{(2)}(z_l, z_m) \end{pmatrix} \tag{A1.8}$$

which describes the joined propagation of the particles. To find the interplane propagator one has to count all possible paths leading from a site 0 to a site at distance r. Due to the limit $K \to \infty$ the particles move coherently only along the direct path from 0 to r. Any excursion in the lattice takes place incoherently. It is *this* property that causes destructive interference and thus a finite conductivity. In view of this interpretation we divide the path in three parts: (i) coherent propagation from site 0 to site s, (ii) incoherent interplane hopping from s to t, and (iii) coherent propagation from site t to r. Paths (i) and (iii) are simply given by $G^{(2)}(s)$ and $G^{(2)}(r-t)$, respectively. Path (ii) can be directly found from (A1.6):

$$\tilde{H}^{(2)}(r; z_l) = \begin{pmatrix} o(r)\left(\frac{g_{\mathrm{U}}(z_l) g_{\mathrm{U}}(z_m)}{g_{\mathrm{L}}(z_l) g_{\mathrm{L}}(z_m)}\right)^{1/2} & e(r) \\ e(r) & o(r)\left(\frac{g_{\mathrm{L}}(z_l) g_{\mathrm{L}}(z_m)}{g_{\mathrm{U}}(z_l) g_{\mathrm{U}}(z_m)}\right)^{1/2} \end{pmatrix} \times \frac{\left(g_{\mathrm{L}}(z_l) g_{\mathrm{U}}(z_l) g_{\mathrm{L}}(z_m) g_{\mathrm{U}}(z_m)\right)^{(1+r)/2}}{1 - g_{\mathrm{L}}(z_l) g_{\mathrm{U}}(z_l)} K^{-(r+1)}. \tag{A1.9}$$

In $G^{(2)}(r-t)$ and in $\tilde{H}^{(2)}$ the particles propagate simultaneously from one sublattice to the other. Therefore it is sufficient to work with 2×2 matrices, contrary to a more general formalism in which one would need 4×4 matrices. We construct the interplane two-particle propagator as

$$H^{(2)}(r; z_l, z_m) = \sum_{s=0}^{r} \sum_{t=s}^{r} G^{(2)}(s; z_l, z_m) \left(G^{(2)}(0; z_l, z_m)\right)^{-1} \times \tilde{H}^{(2)}(t-s; z_l, z_m) \left(G^{(2)}(0; z_l, z_m)\right)^{-1} G^{(2)}(r-t; z_l, z_m)(2 - \delta_{t,0}). \tag{A1.10}$$

Analogous to the one-particle situation in (A1.5) we have overcounting of locators cancelled by both $\left(G^{(2)}(0; z_l, z_m)\right)^{-1}$.

A simple expression for $H^{(2)}(r; z_l, z_m)$ cannot be found for general r. For $\sigma(\omega)$, however, only the sum over r appears. Furthermore, we have to average over the two sublattices, see (11). Hence, we define

$$H^{(2)}(z_l, z_m) = \frac{1}{2}\sum_r N(r)\mathrm{Tr}\, H^{(2)}(r; z_l, z_m) \tag{A1.11}$$

where the trace refers to the 2×2 matrices. Using (A1.10) and (A1.11) one obtains the formula

$$H^{(2)}(z_l, z_m) = \frac{1}{K}\frac{1}{(z_l - z_m)^2}\frac{[g_U(z_l) - g_U(z_m) + (g_L(z_l) - g_L(z_m))g_U(z_l)g_U(z_m)]}{[1 - g_U(z_l)g_U(z_m)][1 - g_U(z_l)g_U(z_m)]} \times \frac{[g_L(z_l) - g_L(z_m) + (g_U(z_l) - g_U(z_m))g_L(z_l)g_L(z_m)]}{[1 - g_U(z_l)g_U(z_m)g_L(z_l)g_L(z_m)]} \tag{A1.12}$$

and partial-fraction expansion results in (13).

Appendix 2.

Here we show that in the limit of infinite coordination number, $Z \to \infty$, the periodic Bethe lattice is equivalent to a hypercubic lattice with half-elliptic DOS. This statement is true for the thermodynamic properties and for the conductivity.

A2.1. Thermodynamics

For the one-particle properties the equivalence is intuitive since the limit of $Z \to \infty$ ensures a mean-field behaviour: the equations defining the DOS involve only a single site and the rest of the lattice enters only via the DOS. Since both the hypercubic and Bethe lattices are bipartite it is possible to divide each of them into two sublattices such that there is *no* direct hopping or interaction on *one* of the sublattices. In the limit $Z \to \infty$ one is led to the introduction of an energy difference 2Δ between the two lattices and the distinction between the locators g_U and g_L. Equations (4) define Δ self-consistently.

To show how local disorder influences the locators the CPA equations are extended (e.g. [35]) to site-dependent problems

$$1 = \int \mathrm{d}\epsilon\, P(\epsilon)\frac{1}{1 - (\epsilon - \Sigma_i)g_i} \tag{A2.1}$$

where Σ_i is the local self-energy at site i, and g_i the corresponding locator which is in turn calculated from the free locators $g_i^{(0)}$ and the self-energies Σ_i. Indeed, the lattice structure does not enter explicitly.

The dependence of the locators on the energy difference 2Δ is provided for the Bethe lattice by (3) at $\gamma = 0$. The spectral function of g_L is then

$$\rho_L(\omega) = \frac{|\omega - \Delta|}{2\pi}\left(\frac{4}{\omega^2 - \Delta^2} - 1\right)^{1/2}. \tag{A2.2}$$

The same result is obtained by inverting the 2×2 matrix

$$-\begin{pmatrix} \epsilon(k) - z & \Delta \\ \Delta & -\epsilon(k) - z \end{pmatrix}^{-1} = \begin{pmatrix} g_{k,k} & g_{k,k+Q} \\ g_{k,k+Q} & g_{k+Q,k+Q} \end{pmatrix} \tag{A2.3}$$

with $g_{k,k'}$ being the propagator from k to k'. This corresponds to the hypercubic problem. The vector Q is the nesting vector $(\pi, \pi, \ldots, \pi)^{\mathrm{T}}$. The locator of the L lattice is then given by

$$g_{\mathrm{L}}(z) = \int \frac{\mathrm{d}^d k}{(2\pi)^d}(g_{k,k} - g_{k,k+Q}) = \int \mathrm{d}\epsilon \rho_0(\epsilon) \frac{z + \epsilon - \Delta}{z^2 - \epsilon^2 - \Delta^2}. \tag{A2.4}$$

If the distribution ρ_0 of the $\epsilon(k)$ is $\sqrt{4-\epsilon^2}/2\pi$ the resulting spectral function of g_{L} is *identical* to the one in (A2.2). The combined situation with disorder and symmetry breaking is included by allowing for a frequency-dependent Δ in (A2.3), and by passing from ω to $\omega - \Sigma(\omega)$, where $\Sigma(\omega)$ is the self-energy averaged over the two sublattices. On the level of the thermodynamic properties the proof of our assertion is thereby completed. In the limit $Z \to \infty$ considering the Bethe lattice is equivalent to considering a hypercubic lattice with a half-elliptic DOS.

A2.2. Transport

The equivalence of the conductivity on the two lattices is the more interesting statement since it is less intuitive. We use the current–current response function $\chi^{jj}(\omega)$ defined as $\chi^{\rho\rho}(\omega)$ in (8) (see also [35,36]) and

$$\sigma(\omega) = \sigma_1(\omega) + \sigma_2(\omega) \tag{A2.5}$$

where

$$\sigma_1(\omega) = \frac{\mathrm{i}e^2}{\omega} \int_{\mathrm{BZ}} \frac{\mathrm{d}^d k}{(2\pi)^d} \partial_{k_x}^2 \epsilon(k) \langle \hat{n}_k \rangle \tag{A2.6a}$$

$$\sigma_2(\omega) = \frac{\mathrm{i}e^2}{\omega} \chi^{jj}(\omega). \tag{A2.6b}$$

Let $\Sigma_{\mathrm{U}}(z_m)$ and $\Sigma_{\mathrm{L}}(z_m)$ be the complete local self-energies on the two sublattices; we introduce $\tilde{\Delta}_m := (\Sigma_{\mathrm{U}} - \Sigma_{\mathrm{L}})/2$ and $w_m := z_m - (\Sigma_{\mathrm{U}} + \Sigma_{\mathrm{L}})/2$. In the limit $Z \to \infty$ the current–current response function, which is of order $1/Z$, is given by the dressed bubble only since all other diagrams either vanish faster than $1/Z$ or are identical to zero due to the parity of the current vertices [25]. With the use of (A2.3) we find therefore

$$\chi^{jj}(\omega) = \frac{1}{\beta} \sum_m \int_{\mathrm{BZ}} \frac{\mathrm{d}^d k}{(2\pi)^d} \frac{\big(\partial_{k_x}\epsilon(k)\big)^2 (w_m + \epsilon(k))\big(w_l + \epsilon(k)\big)}{\big(w_m^2 - \epsilon^2(k) - \tilde{\Delta}_m^2\big)\big(w_l^2 - \epsilon^2(k) - \tilde{\Delta}_l^2\big)}\Bigg|_{(z_m - z_l) \to \mathrm{i}(\omega + \mathrm{i}0+)}$$
$$+ \frac{1}{\beta} \sum_m \int_{\mathrm{BZ}} \frac{\mathrm{d}^d k}{(2\pi)^d} \times \frac{\big(\partial_{k_x}\epsilon(k)\big)\big(\partial_{k_x}\epsilon(k+Q)\big)\tilde{\Delta}_m \tilde{\Delta}_l}{\big(w_m^2 - \epsilon^2(k+Q) - \tilde{\Delta}_m^2\big)\big(w_l^2 - \epsilon^2(k+Q) - \tilde{\Delta}_l^2\big)}\Bigg|_{(z_m - z_l) \to \mathrm{i}(\omega + \mathrm{i}0+)}. \tag{A2.7}$$

In leading order $1/Z$ the expression $\big(\partial_{k_x}\epsilon(k)\big)^2 = 4\sin^2(k_x)/Z$ can be substituted by its average $2/Z$ (the hopping is set to $1/\sqrt{Z}$). Exploiting the perfect-nesting property $\epsilon(k+Q) = -\epsilon(k)$ we obtain

$$\chi^{jj}(\omega) = \frac{2}{Z\beta} \sum_m \int \mathrm{d}\epsilon \rho_0(\epsilon) \frac{(w_m + \epsilon)(w_l + \epsilon) - \tilde{\Delta}_m \tilde{\Delta}_l}{(w_m^2 - \epsilon^2 - \tilde{\Delta}_m^2)(w_l^2 - \epsilon^2 - \tilde{\Delta}_l^2)}\Bigg|_{(z_m - z_l) \to \mathrm{i}(\omega + \mathrm{i}0+)} \tag{A2.8}$$

which can be decomposed in partial fractions, each of which yielding a one-particle Green function, i.e.

$$\chi^{jj}(\omega) = \frac{2}{Z\beta}\sum_m \eta[\kappa_m g_U(z_m) + \kappa_l g_U(z_l) + \lambda_m g_L(z_m) + \lambda_l g_L(z_l)]\Big|_{(z_m - z_l)\to i(\omega+i0+)} \tag{A2.9}$$

with

$$\eta := (w_l^2 - w_m^2 - \tilde{\Delta}_l^2 + \tilde{\Delta}_m^2)^{-1} \tag{A2.10a}$$

$$\kappa_m := \tfrac{1}{2}(w_l + w_m - \tilde{\Delta}_l - \tilde{\Delta}_m) \qquad \kappa_l = -\kappa_m \tag{A2.10b}$$

$$\lambda_m := \tfrac{1}{2}(w_l + w_m + \tilde{\Delta}_l + \tilde{\Delta}_m) \qquad \lambda_l = -\lambda_m. \tag{A2.10c}$$

In (A2.9) the shape of the DOS has *not* yet entered at all *nor* has the disorder distribution $P(\epsilon)$ been specified. If we now choose ρ_0 and $P(\epsilon)$ to be half-elliptic, as in the main part of the paper, we may refer to the equivalent thermodynamic result (3) (see also (A2.1)) yielding

$$\sigma_2(\omega) = \frac{ie^2}{Z\beta\omega}\sum_m \left(\frac{2 + g_U(z_m)g_L(z_l) + g_L(z_m)g_U(z_l)}{1 - g_U(z_m)g_L(z_m)g_U(z_l)g_L(z_l)} - 2\right)\Big|_{(z_m - z_l)\to i(\omega+i0+)}. \tag{A2.11}$$

By a similar line of argument $\sigma_1(\omega)$ is found:

$$\sigma_1(\omega) = -\frac{2ie^2}{Z\beta\omega}\sum_m \frac{g_U(z_m)g_L(z_m)}{1 - g_U(z_m)g_L(z_m)}. \tag{A2.12}$$

The last two equations (A2.11) and (A2.12) together give exactly the same dynamical conductivity as do (12) and (13), thereby concluding our argument.

Appendix 3.

In this appendix we verify the f-sum rule for the conductivity [37]

$$\int_{-\infty}^{\infty} \sigma_{xx}(\omega)\mathrm{d}\omega = -\pi e^2\langle \hat{T}_{xx}\rangle. \tag{A3.1}$$

The subscript xx indicates the direction in which the diagonal conductivity σ_{xx} is measured and which part of the kinetic energy per site $\hat{T}$ is included. Making use of the Kramers–Kronig relation [35] the LHS of (A3.1) can be expressed as $-i\pi \lim_{\omega\to\infty} \omega\sigma(\omega)$. Examining (12) and (13) it can be seen that only the first two terms of $H^{(2)}$ will contribute in the limit $\omega \to \infty$. Furthermore their contribution is identical. We obtain for the LHS of (A3.1)

$$\int_{-\infty}^{\infty} \sigma_{xx}(\omega)\mathrm{d}\omega = -\frac{2\pi e^2}{K\beta}\sum_m \frac{g_U(z_m)g_L(z_m)}{1 - g_U(z_m)g_L(z_m)}. \tag{A3.2}$$

To compute the RHS we recall that the Green function corresponding to direct interplane hopping is given in (A1.4). Hence

$$\langle \hat{c}_{il}^{+}\hat{c}_{i(l+1)}\rangle = -\frac{1}{\sqrt{K}\beta}\sum_m \frac{g_U(z_m)g_L(z_m)}{1 - g_U(z_m)g_L(z_m)} \tag{A3.3}$$

where $\hat{c}_{il}^{+}$ is the creation operator on site i on the Bethe lattice l and $\hat{c}_{i(l+1)}$ is the annihilation operator on site i on the adjacent Bethe lattice $l+1$. The matrix element for the hopping and its complex conjugate is $-1/\sqrt{K}$, which yields

$$\langle \hat{T}_{xx} \rangle = \frac{2}{K\beta} \sum_m \frac{g_U(z_m) g_L(z_m)}{1 - g_U(z_m) g_L(z_m)}. \tag{A3.4}$$

Inserting (A3.4) and (A3.2) into (A3.1) easily proves that the f-sum rule for conductivity is fulfilled. The limit of infinite coordination number conserves sum rules, as was to be expected since sum rules are equalities that hold in every dimension (or for every branching ratio) so that they can be extended to $Z \to \infty$ if continuity is provided.

References

[1] Ma M 1982 *Phys. Rev.* B **26** 5097
[2] Finkel'shteĭn A M 1983 *Sov. Phys.–JETP* **57** 97
[3] Castellani C, Di Castro C, Lee P A and Ma M 1984 *Phys. Rev.* B **30** 527
Castellani C, Di Castro C and Grilli M 1986 *Phys. Rev.* B **34** 5907
Castellani C, Kotliar G and Lee P A 1987 *Phys. Rev. Lett.* **59** 323
[4] Zimanyi G T and Abrahams E 1990 *Phys. Rev. Lett.* **64** 2719
[5] Dobrosavljević V and Kotliar G 1992 *Rutgers University preprint*
[6] Finkel'shteĭn A M 1984 *Z. Phys.* B **56** 189
[7] Castellani C, Di Castro C, Lee P A, Ma M, Sorella S and Tabet E 1984 *Phys. Rev.* B **30** 1596; 1986 *Phys. Rev.* B **33** 6169
[8] Milovanović M, Subir Sachdev and Bhatt R N 1989 *Phys. Rev. Lett.* **63** 82
[9] Belitz D and Kirkpatrick T R 1990 *Physica* A **167** 259
Kirkpatrick T R and Belitz D 1990 *Phys. Rev.* B **41** 11082
[10] Lee P A and Ramakrishnan T V 1985 *Rev. Mod. Phys.* **57** 287
[11] Janiš V and Vollhardt D 1992 *Phys. Rev.* B **46** 15712
[12] Vlaming R, Uhrig G S and Vollhardt D 1992 *J. Phys.: Condensed Matter* **4** 7773
[13] Metzner W and Vollhardt D 1989 *Phys. Rev. Lett.* **62** 324
[14] Vollhardt D 1992 *Correlated Electron Systems* ed. V J Emery (Singapore: World Scientific)
[15] Rozenberg M J, Zhang X Y and Kotliar G 1992 *Phys. Rev. Lett.* **69** 1236
[16] Georges A and Kotliar G 1992 *Phys. Rev.* B **45** 6479
[17] Georges A and Krauth W 1992 *Phys. Rev. Lett.* **69** 1240
[18] Pruschke T, Cox D L and Jarrell M 1992 *Ohio preprints I and II*
[19] Cullen J R and Callen E 1970 *J. Appl. Phys.* **41** 879; 1971 *Phys. Rev. Lett.* **26** 236
[20] des Cloizeaux J and Gaudin M 1966 *J. Math. Phys.* **7** 1384
[21] Yang C N and Yang C P 1966 *Phys. Rev.* **150** 321, 327
[22] Shankar R 1990 *Nucl. Phys.* B **330** 433; 1991 *Physica* A **177** 530
[23] Müller-Hartmann E 1989 *Z. Phys.* B **74** 507
[24] Vlaming R and Vollhardt D 1992 *Phys. Rev.* B **45** 4637
[25] Khurana A 1990 *Phys. Rev. Lett.* **64** 1990
[26] Economou E N 1979 *Green's Functions in Quantum Physics* (Berlin: Springer)
[27] Efetov K B 1987 *Sov. Phys.–JETP* **65** 360
[28] Elliott R J, Krumhansl J A and Leath P L 1974 *Rev. Mod. Phys.* **46** 465
[29] Ihle D and Lorenz B 1986 *J. Phys. C: Solid State Phys.* **19** 5239
[30] Tsuda N, Nasu K, Yanase A and Sitatori K 1991 *Electronic Conduction in Oxides* (Berlin: Springer)
[31] Anderson P W 1990 *Phys. Rev. Lett.* **65** 2306; 1990 *Int. J. Mod. Phys.* B **4** 181
[32] Mielke A 1990 *J. Stat. Phys.* **62** 509
[33] Thomas G A, Orenstein J, Rapkine D H, Capizzi M, Millis A J, Bhatt R N, Schneemeyer L F and Waszczak J V 1988 *Phys. Rev. Lett.* **61** 1313
[34] Strack R and Vollhardt D 1991 *J. Low Temp. Phys.* **84** 357
[35] Rickayzen G 1980 *Green's Functions and Condensed Matter* (New York: Academic)
[36] Mahan G D 1990 *Many Particle Physics* 2nd ed (New York: Plenum)
[37] Baeriswyl D, Gros C and Rice T M 1987 *Phys. Rev.* B **35** 8391